た。荷重値の相違による測定結果は、10,15,20,25,30Nの荷重にてそれぞれET変形角は0.095, 0.131, 0.193, 0.229, 0.279であった。荷重値とET変形角の相関はR= 0.9969と高い相関を示した。(図4)

(力学特性の検出精度の評価測定)

8名9肢に対する臨床測定では測定回数(患者来院1回で1測定と計算)は、のべ 61 回であった。

症例 1 はギプス治療が行われた症例であるが、受傷後 4 週と早時期からの測定で、ET 変形角も約1度と大きな値が検出された。受傷後4週では血腫や繊維性組織による弱い結合がほとんどであり、レントゲンにても仮骨はほとんど確認出来ない。その後、レントゲンでは19週までレントゲン透過性が低下し、認識される仮骨部分の領域が増した。その後、仮骨領域の透過性はさらに低下し周囲の皮質部分に近づいた。このレントゲンの推移は、一般に整形外科診療で骨形成が良好に進行していると判断される。測定された ET 変形角では 19 週まで急激に減少した期間が、レントゲンより推定される仮骨形成期にあたると考えられた。ET 変形角はその後も減少を続けるが 21 週以降ではついには健常側より少なくなる。レントゲンにおいて 26 週以降では、仮骨部の透過性変化はほぼ判別困難となるが、ET 変形角はその後も減少が見られていた。この症例の ET 変形角は指数関数的に有意に減少していた。これらの結果より、ET 計測により剛性の変化が定量評価可能であった。(図5)

症例2もギプス治療が行われた症例で, レントゲンでは経時的に斜骨折間の透過性はやや減少していたが癒合程度の推測は症例1より困難であった。測定されたET変形角では13週まで急激に減少し、その後も減少を続け指数関数的に有意な減少であった。22 週以降では健常側より変形角が少なくなっており、症例1と同様の経時変化を呈していた。

症例3は脛骨骨幹部に骨軸長約 10cm の腸骨を移植された症例で、ET 測定開始時の術後8ヶ月の時点で骨癒合は得られていたが、移植された腸骨は前方凸の湾曲した骨で短径も健常脛骨に比して小さいため、曲げに対する強度が不十分であることが予想された。そのため、受診時も骨幹部のみを保護するシリンダー状の装具を使用していた。レントゲンでは、経過に伴い腸骨が接合された近遠位の断端の短径がわずかに増大していく様子が見られ、接合部に対するメカニカルストレスに呼応した骨形成が行われたと推測された。しかし、レントゲン撮影条件が少しでも異なると骨幅の増減の判断は難しく、さらに形状が正常の骨と異なり、レントゲンからの強度の推測は困難であった。ET 測定では、8ヶ月から23ヶ月にかけて健常に対し5倍から2倍程度まで指数関数的に有意に変形角が減少していくことが捉えられ、力学特性の変化が定量評価可能であった。

症例4は骨癒合が得られたと判断され、創外固定器抜去後の測定であった。ET 変形角は開始時より健常側の2倍程度であり、その後の減少変化も軽微であり指数関数的に有意な減少は見られなかった。レントゲンでは明らかな変化として捉えることは出来なかった。

症例5は髄内釘による手術症例であるが、髄内釘は骨髄内に挿入され骨折部を貫通するが、髄内釘により髄腔が完全に占拠されるわけではなく近遠位の 2 本ずつのスクリューにより固定される。よって、骨折部が手術により完全に固定されているわけではなく、特に曲げや回旋方向のストレスに対しては骨癒合が得られるまでは十分な強度を有しているとはいえない。測定開始時の4週では健常側の4倍程度のET変形角が測定され、経過に伴いET変形角は指数関数的に有意に減少した。内固定材を用いた手術症例においても、力学特性の変化が定量評価可能であった。

症例6も髄内釘による手術症例であるが、左右肢の症例である。この左右の骨折はレントゲン上、形態が異なり左は横骨折なのに対し、右はやや斜骨折で骨折部に第 3 骨片(遊離している骨)が存在している。このため、手術後も右側は安定性に欠けることが予想された。実際、測定開始時の 5 ヶ月時において患者は T 字杖歩行を行っていたが、右側の骨折部には歩行時痛を伴っていた。ET 測定の結果は、両側ともレントゲンにおける仮骨の経時変化に対応し、ET 変形角は減少が見

られたが、右側は常に左側の ET 変形角より大きく、この左右差も ET 計測において定量評価可能であった。

症例7は髄内釘による手術症例であるが、手術後 5 年を経過した症例で、現在独歩は可能であるが長時間の歩行や走行にて骨折部に痛みが伴うため ET 測定を行った。レントゲンでは Hypertrophic Nonunion（骨形成は見られるが骨癒合が得られていない骨癒合不全）の様態を示していたが、レントゲンの経時変化から骨癒合の進行が全くないとの判断は難しかった。ET 測定の結果、3 回の測定ではあるが、常に健常側の 5 倍以上の ET 変形角を示し指数関数的に優位な減少は見られなかった。ET 計測により、定量的に剛性の変化がないことが評価可能となった。

症例8は金属プレートによる手術症例であるが、レントゲンでは骨折線が骨長軸方向に 80mm に及ぶ斜骨折で、192mm の長いプレートにより固定された。骨折線が広範に及ぶことと、高齢であることから骨癒合の遷延が予想された症例であるが、レントゲンでも仮骨形成は測定期間において明らかな変化がみられなかった。ET 測定では、0.265 度と金属プレートの変形角が検出可能でその後、わずかな ET 変形角の減少が検出されたが指数関数的に有意な減少は見られなかった。ET 測定による定量評価により緩徐な剛性の変化が検出可能であった。

D. 考察

（脛骨モデル測定実験）

3 点曲げ試験に用いた骨モデルの曲げ剛性が健常骨の曲げ剛性に近似していることは Cristofolini らによる摘出脛骨とこのモデル脛骨の曲げ試験での比較実験により明らかにされたものである。この健常骨モデルの 3 点曲げ計測により ET 変形角が検出可能か測定した結果、ET 変形角は 0.1145 度と金属平板における ET 変形角の精度である 0.0015 度を十分上回るものであり、3 点曲げにおける 25N 荷重での測定は骨の曲げ剛性を十分検出可能な測定法であると考えられた。荷重部分の断面積や材質にも依存するが 25N の荷重量は感覚的には親指で軽く押す程度の荷重であり、全く疼痛を与えない非侵襲といえる程度の荷重量である。

この測定された角度が真に荷重により生じた超音波ビーム方向の角度変化であるか検討した結果、ビーム垂直方向へは 10 μm程度の併進であり、その場合の測定誤差はさらに小さいものであることが明らかにされ、ET 変形角はほぼ超音波ビーム方向の角度変化であるといえた。

（臨床測定方法の検討）

健常骨測定の結果，模擬骨同様に変形角が検出され，臨床においても 3 点曲げ計測が可能であることが示された。

荷重値の相違による ET 変形角を測定した計測では、荷重値とET変形角に非常に高い相関（R= 0.9969）が見られ、10～30N の荷重範囲では変形角は弾性的に起きていることを示していた。このことは今後、症例間で荷重量の異なる条件で測定を行った際、測定距離・荷重量を算出し Stiffness として一般化出来る可能性を示した。今後は骨粗鬆症の患者を対象に測定を実施し健常者との変形角の比較・患者間での比較を行い DEXA 等との相関を調べていく。

（力学特性の検出精度の評価測定）

レントゲン画像・臨床診断上に良好な骨癒合の進行が類推された症例ではいずれも ET 計測により得られた変形角度は指数関数的に減少が見られ健常側の変形角度に近づいた。角度変化が指数関数様の減少を示していた結果は既存の骨折における剛性変化の評価を試みた測定法と一致しており，ET 法により剛性変化が検出出来ていたことが裏付けられる。Jernberger は脛骨前内側面の中心部・近遠位部に 3 本のピンを局所麻酔下に刺入し、これらをロッドにて連結し、中心部のピンを押し込みその荷重量と変位量を計測する手法を考案した。彼はこの測定を保存療法を行った脛骨骨幹部骨折 40 症例に対し測定を行い、また同時に健常側にもピンを刺入し、測定を行い比較した。こ

の測定は骨の両端をピン固定して荷重による撓み量を計測する手法であり、非侵襲的方法であるとは言えないがその結果、レントゲンにて骨癒合過程が良好と判断される症例において、5kgf の荷重に対するピンの変位量は経時的に減少し健常側に近づいた。これらの測定における骨癒合曲線は、受傷 6 週からの計測結果であったが、測定初期において変位量は急激に減少し 16～22 週程度の時期からは緩徐な減少を示す指数関数的減少を示す症例がほとんどであった。

これらの結果からＥＴ法により骨癒合変化における剛性変化が検出可能であることが示されたが，今後は骨粗鬆症における薬剤効果を検討するための経時測定を行っていく。しかし，この測定での力学特性の変化はさらに微小となることが予測されるためより高精度な測定が可能となるよう測定システムの向上を図る必要がある。

3点曲げ測定の今後の課題

この 3 点曲げによるET計測により、既存の方法では成し遂げることが出来ていない骨の力学特性を定量的に検出可能であったが，より高精度な測定を行うためいくつかの課題が残されている。

8 名 9 肢に対する臨床測定の結果では ET 解析不能となった施行が少なからず存在し、これらの多くは荷重時による波形の形態変化に起因するものであった。波形の形態変化の原因としては取得波形の Amplitude が低い事、若しくは波形取得面が大きく変化していることが挙げられる。Amplitude が低いことは測定開始時に波形データから確認可能であるが、測定面が曲面になっている症例が多かった。もう一つの原因である波形取得面の変化は、荷重方向以外に併進を起こしている事を示し測定中の患者の体動、若しくは固定が不十分で荷重により下腿が回旋したことが考えられた。現在の固定冶具の固定力は陰圧による密着力のみでそれも全面での密着ではないため今後の固定法の改良が必要と考えられた。

また、3 点曲げとしているが、この支点も現在では明確ではない。現在、これらの問題を改善するために新たな 3 点曲げ冶具を作成中である。この冶具は脛骨が隣接する腓骨頭(脛骨と腓骨の連結近位部)と外果を支点とし、荷重を垂直に受ける方式である。これにより支点位置が明確になり荷重による回旋も減少すると考えられる。

また、荷重方法についても現在の徒手的な方法であると、荷重方向と荷重速度のコントロール精度に問題が残されるため粘弾性測定も可能な機械的荷重方法を考案している。

また、測定部位についても、大腿骨・橈骨での測定を計画しておりその計測を可能とするプローブ・固定冶具の検討・製作を行っている。

E．結論

現在、骨粗鬆症における骨強度測定はそのほとんどが骨密度測定により代用されている。しかし、骨密度測定が強度と必ずしも相関しないことはすでに明らかにされている。これに対し ET 法は骨の荷重に対する変形そのものを検出し測定する手法であるため力学特性を正確に検出可能な方法として優れていると考えられる。

本研究によりET 法を用いた 3 点曲げにおけるモデル骨・健常骨における測定は骨の曲げ剛性を十分検出可能な測定法であると考えられた。また、骨折症例での測定において骨の力学特性の変化を経時測定可能であった。このことから ET 法により骨の Mechanical Property を非侵襲に高精度に検出可能であることが確かめられ骨粗鬆症など易骨折性を有する疾患の骨強度測定の可能性が示された。

既存の方法において非侵襲に骨の力学的特性を高精度に定量評価出来たものはなくこの ET 測定により初めて測定が可能となった。今後，骨粗鬆症の骨の計測を行うが，それに向け現在固定時具・荷重機構の改良を行い再現性・精確性の向上を図っている。また、測定部位の汎用性を持たせるために新たな骨計測用プローブを開発している。

F．研究発表

7．論文発表

Matsuyama J. Ohnishi I. Sakai R. Suzuki H.

Harada A. Bessho M. Matsumoto T. Nakamura K.
A New Method for Measurement of Bone Deformation by Echo Tracking
Medical Engineering & Physics (In Press)

Ohnishi I, Kurokawa T, Sato W, Okazaki H, Nakamura K, Measurement of the tensile forces during bone lengthening.
Clinical Biomechanics, 20 (4), 421-427, 2005.

Kazuhiro Imai, Isao Ohnishi, Masahiko Bessho, Kozo Nakamura. Nonlinear Finite Element Model Predicts Vertebral Bone Strength and Fracture Site. Spine (in press)

8. 学会発表
松山 順太郎・大西 五三男・酒井 亮一・鈴木 浩之・原田 烈光・大橋 暁・別所 雅彦・中村 耕三. 超音波エコートラッキング法を用いた骨の非侵襲変形計測法の基礎研究 第20回日本整形外科基礎学術集会 2005.

Matsuyama J, Ohnishi I, Sakai R, Suzuki H , Harada A, Bessho M, Matsumoto T, Nakam ura, K.
A new method for accurate measurement of bone deformation with echo tracking. The 52nd annual meeting of the Orthopaedic Research Society, 2006 Chicago

M. Bessho, I Ohnishi, T.Kageyama, Oshida, T. Suwabe, K Nakamura, Prediction of strang th and strain of thebone with a defect by a C T based finite element method. 51th Meeting o f Orthopadic Research Society. 2005

Bessho M, Ohnishi I, Matsuyama J, Matsumoto, T, Nakamura, K. Prediction of strength and strain of the proximal femur by a CT based finite element method. The 52nd annual meeting of the Orthopaedic Research Society, 2006 Chicago

G. 知的財産権の出願・登録状況（予定を含む。）
2. 特許取得

1、特願2003-91097 超音波診断装置
2、特願2003-403086 超音波診断装置
3、特願2005-103031 超音波診断装置
4、出願10/951,322
ULTRASONIC DIAGNOSTIC APPARATUS
5、出願 04022856.1
ULTRASONIC DIAGNOSTIC APPARATU

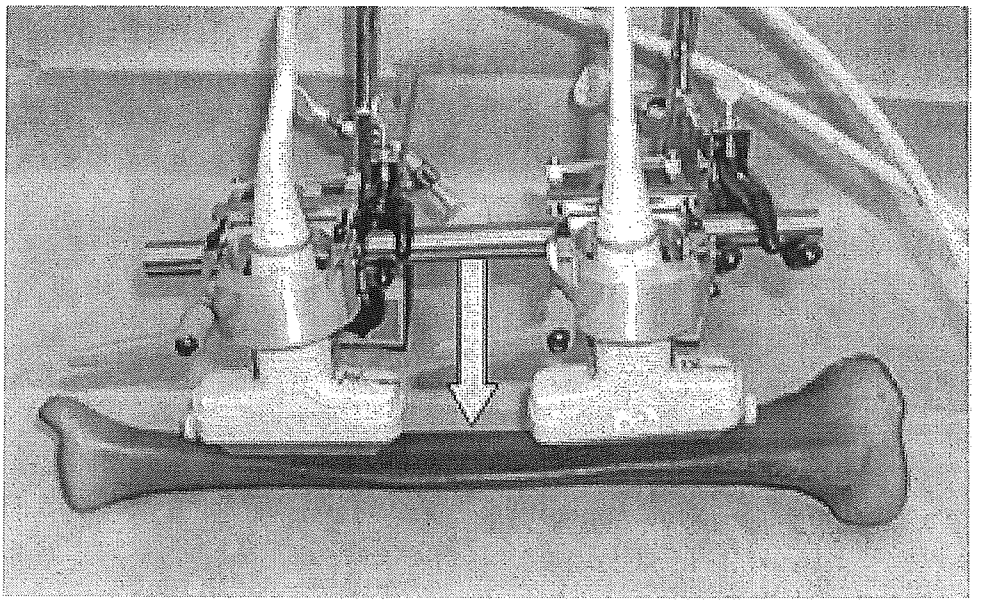

図1　脛骨モデルによる3点曲げ測定法の検証実験写真

脛骨モデルの前内側面が上面となるように置き，前内側面に垂直になるようフォースゲージにて25Nの荷重を加えた。近遠位のプローブはマグネット式の3関節アームで保持し，前内側面の骨幅中心を通る軸上で前内側面に垂直になるよう設置した。

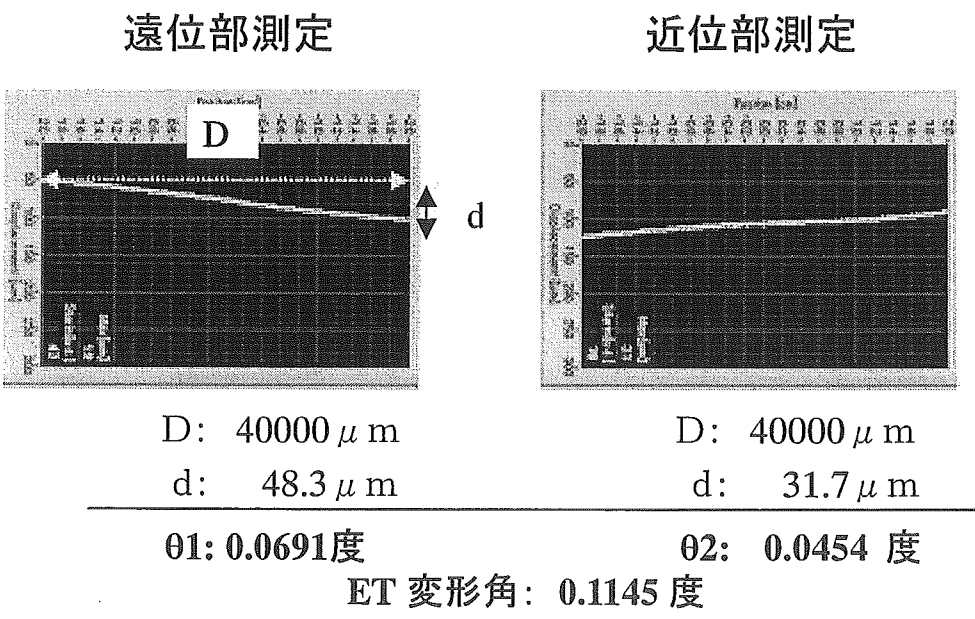

図 2　脛骨モデルによる 3 点曲げ測定法の測定結果

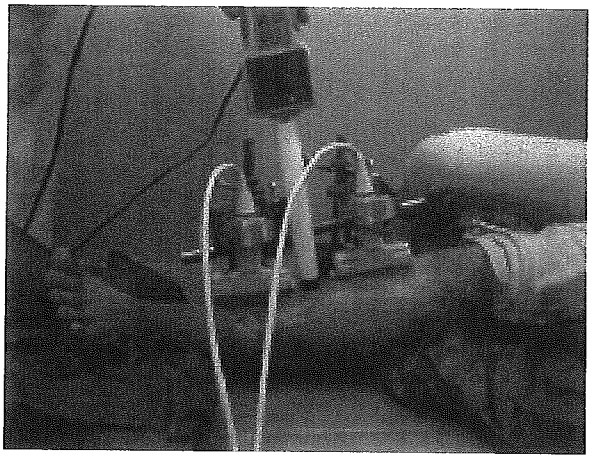

図 3　臨床 3 点曲げ計測法

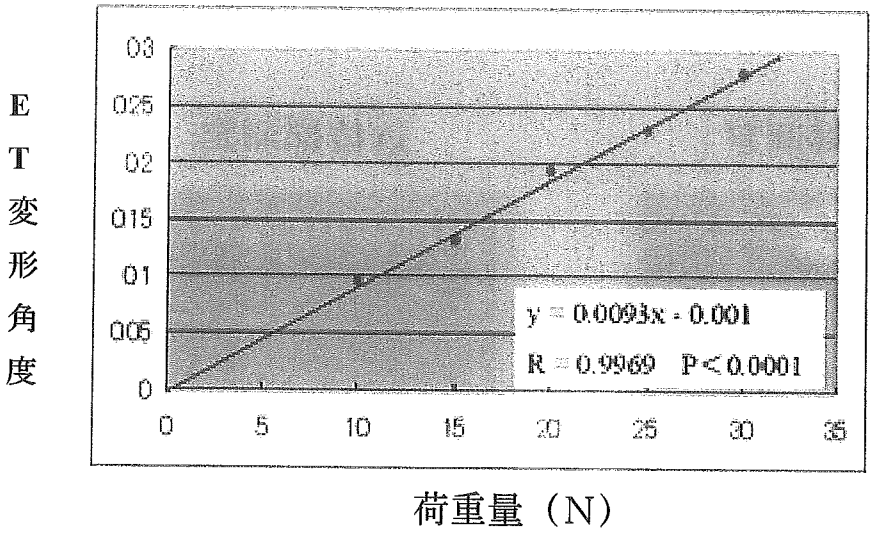

図 4　荷重値の相違による ET 変形角臨床測定

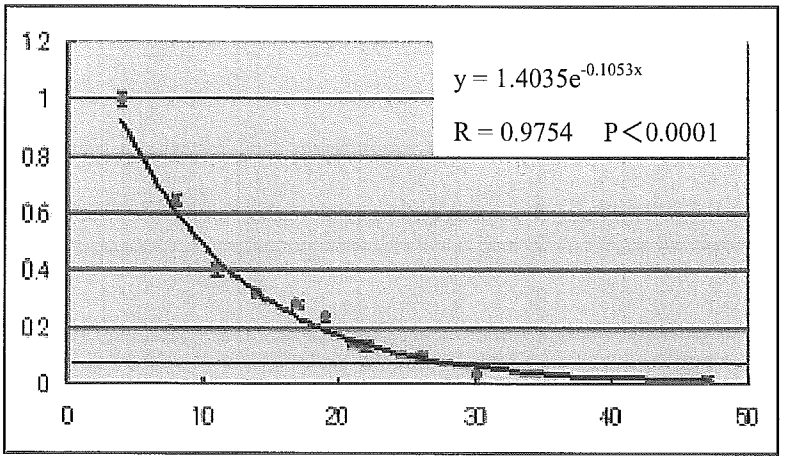

図5　症例1のET変形角経時変化(指数近似と相関係数)

書籍

著者氏名	論文タイトル名	書籍全体の編集者名	書籍名	出版社名	出版地	出版年	ページ

雑誌

発表者氏名	論文タイトル名	発表誌名	巻号	ページ	出版年
Matsuyama J. Ohnishi I. Sakai R. Suzuki H. Harada A. Bessho M. Matsumoto T. Nakamura K.	A New Method for Measurement of Bone Deformation by Echo Tracking	Medical Engineering & Physics			In press
Ohnishi I, Kurokawa T, Sato W, Okazaki H, Nakamura K.	Measurement of the tensile forces during bone lengthening.	Clinical Biomechanics	20 (4)	421-427	2005.
Kazuhiro Imai, Isao Ohnishi, Masahiko Bessho, Kozo Nakamura.	Nonlinear Finite Element Model Predicts Vertebral Bone Strength and Fracture Site.	Spine			In press

Available online at www.sciencedirect.com
SCIENCE DIRECT®
ELSEVIER
Medical Engineering & Physics xxx (2005) xxx–xxx
Medical Engineering & Physics
www.elsevier.com/locate/medengphy

Technical note

A new method for measurement of bone deformation by echo tracking

J. Matsuyama [a], I. Ohnishi [a,*], R. Sakai [b], H. Suzuki [b], A. Harada [b], M. Bessho [a], T. Matsumoto [a], K. Nakamura [a]

[a] *Department of Orthopaedic Surgery, University of Tokyo, 7-3-1 Hongo, Bunkyo-ku Tokyo 113-0033, Japan*
[b] *Research Laboratory, Aloka Co. Ltd., Tokyo, Japan*

Received 18 February 2005; received in revised form 14 August 2005; accepted 27 September 2005

Abstract

No method has been available to noninvasively detect bone deformation or strain under loading in vivo. We focused on ultrasonic measurement of the displacement at a certain point on a bone using the echo-tracking method (ET). To develop a method that can noninvasively detect bone deformation in vivo, a preliminary investigation was performed.

We investigated the accuracy of measuring displacement with our echo tracking system by using a flat metal panel and found that the method could measure displacement with a precision of a few microns.

A three-point bending test of a porcine tibia with both ends fully constrained was performed to measure bone surface displacement, and simultaneous measurement of the surface strain was done using two strain gauges. The correlation between the displacement measured by ET and the strain gauge readings was completely linear ($r=0.999$), showing that the method could precisely detect bone deformation. The loads versus displacement curves obtained with cyclic loading were typical hysteresis loops that showed viscoelastic properties of the measured bone.

We also improved a multi-ET system capable of simultaneously tracking multiple points to detect deformation of the bone surface. Measurement by this echo tracking system was also compared with strain gauge readings during a three point bending test with both ends of the tibia supported. The linearity of both methods was very high ($r=0.998$). Our ET method might have considerable potential for noninvasive measurement of bone viscoelasticity and plasticity.

Keywords: Echo tracking; Bone deformation; Noninvasive measurement; Bone strain

1. Introduction

Bone is a self-repairing structural material that adapts its mass, shape, and properties to changes in mechanical requirements and tolerates voluntary physical activity throughout life without breaking or causing pain. Quantifying the mechanical inputs into bone is important for understanding the form and function of the skeleton. The forces applied to each bone at the organ level must be translated to the cellular level and then somehow play a role in the maintenance and adaptation of bone tissue [1–3].

Bone fails if subjected to a force exceeding its strength, but even physiological loading during daily activities causes deformation depending on a bone's mechanical properties. Determining the extent of which deformation normally occurs should help to elucidate the mechanotransduction mechanism in bone [4]. Therefore, it is important to be able to quantitatively measure the extent of bone deformation or strain under loading.

To date, many methods have been tried to detect bone deformation under a load [5,6]. A strain gauge is a device that measures the deformation of materials to which it is attached, and this has been the method used to quantify bone strains in vivo. The strain gauge is thus the gold standard for measuring bone deformation in vivo and this device has provided much useful data [7,8]. However, measurement with strain gauges requires invasive exposure of a site for attachment to the bone surface. To date, no method has been available to noninvasively detect bone deformation or strain under loading.

* Corresponding author. Tel.: +81 3 5800 8656; fax: +81 3 3818 4082.
E-mail address: OHNISHII-DIS@h.u-tokyo.ac.jp (I. Ohnishi).

1350-4533/$ – see front matter © 2005 IPEM. Published by Elsevier Ltd. All rights reserved.
doi:10.1016/j.medengphy.2005.09.005

To overcome the above-mentioned limitations in the measurement of bone deformation, we focused on the use of ultrasound because of its noninvasiveness. Ultrasonic waves can penetrate soft tissues and visualize the bone surface. In addition, precise measurement of the displacement of a specific point can be achieved by the echo-tracking method. The echo tracking method measures extent of the displacement by tracking the initialized phase pattern of the radio frequency (RF) echo signal. Hokanson et al. [9] have developed an ultrasonic echo-tracking device that allows arterial wall motion to be measured transcutaneously using the standard pulse reflection technique. The motion of the echoes from the arterial wall was tracked by a gated threshold detector and converted into an analog output suitable for recording. The echo tracking method currently used for measuring arterial wall motion has an accuracy of one sixteenth of a wavelength which is an accuracy of 13 μm at every 1 mm/s with a 7.5 MHz probe [10].

Utilizing such an echo tracking method, it is possible to accurately and dynamically detect the displacement of a specific point on the surface of a bone. By detecting the displacement of multiple points on the bone surface under dynamic loading, it may be possible to detect dynamic bone deformation. The final goal of our investigations is to develop a method that can noninvasively detect bone deformation under loading in vivo by ultrasonic echo tracking method. For this purpose, a preliminary study was performed to confirm that our method had sufficient precision to detect bone surface deformation by conducting in vitro three-point bending tests of bone specimens.

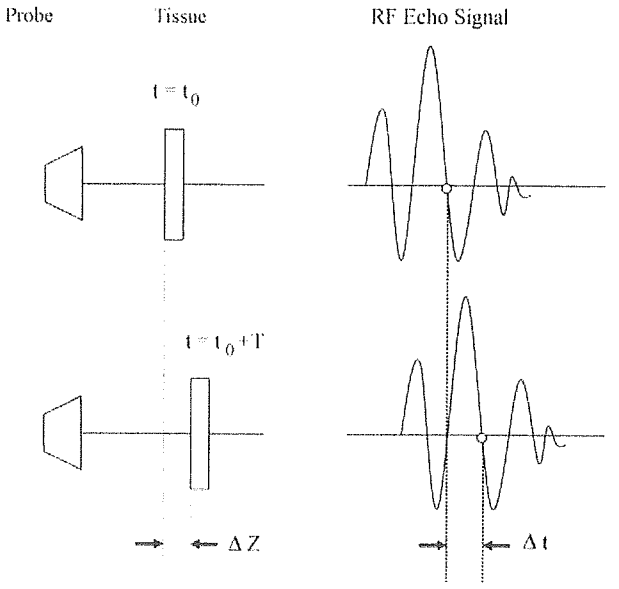

Fig. 1. A diagram of the principal of echo tracking method. Tissue at a certain depth is displaced at time ($t=t_0$) so that it moves away from the probe for a minute distance, ΔZ, during a single cycle of an ultrasonic wave pulse, T. This causes phase delay of a RF echo signal from a tissue for a very short period of time, Δt.

2. Materials and methods

2.1. Echo tracking method

The accuracy of measuring the distance from a probe based on B-mode images depends on the ultrasound wave length and is the order of about 210 μm at a frequency of 7.5 MHz. In contrast, the echo tracking method is a technique measuring minute displacement of a certain point on a tissue with superior accuracy to standard ultrasound by detecting a wave pattern in a RF echo signal reflected from the tissue. For example, it is assumed that a tissue at a certain depth is displaced at time ($t=t_0$), so that it moves away from a probe for a small distance of ΔZ during a single cycle period of an ultrasonic wave pulse, T. This causes phase delay of the RF echo signal from the tissue for a very small period of time, Δt (Fig. 1). The echo tracking method measures extent of the displacement by tracking the initialized phase pattern of the RF echo signal.

We developed the echo tracking system and originally designed the software to utilize the characteristics of the acoustic impedance of bone to accurately measure the displacement on the surface of a bone. A diagram of the echo tracking system specifically designed for bone was shown in Fig. 2. Ultrasound wave was transmitted to the bone surface with a 7.5 MHz linear probe connected to an ultrasonic diagnostic device (SSD-1000, Aloka, Tokyo, Japan). The RF

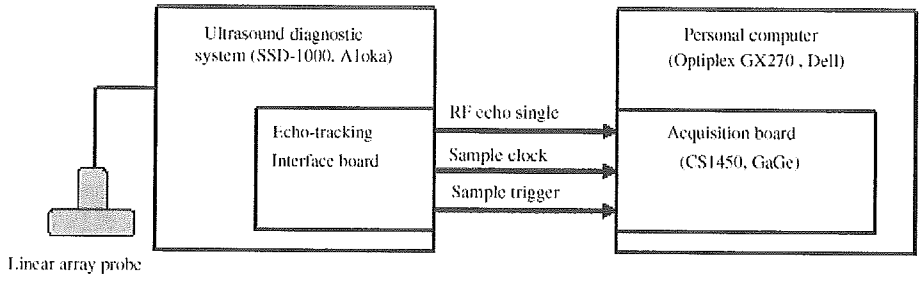

Fig. 2. A block diagram illustrating bone deformation measurement by echo tracking. The RF echo signal is recorded on a personal computer via the echo-tracking interface installed in the ultrasonography device. At the same time, a sample clock signal and sample trigger signal are transmitted to the PC synchronized with a transmit pulse repetition signal.

echo signal reflected from the bone surface was recorded on a personal computer (PC) (Optiplex GX270, Dell, TX, USA) via the echo-tracking interface installed in the ultrasonic diagnostic device. At the same time, a sample clock signal with a frequency of 50 MHz and a sample trigger signal with a frequency of 500 Hz were transmitted to the PC synchronized with a transmitting pulse repetition signal. The analog RF echo signal was converted into a 14-bit digital signal with a sampling frequency of 50 MHz by using a logging board (CS1450, GaGe, Montreal, Canada) installed in the PC and then the data were recorded. The stored RF echo data were interpolated to eight times to allow the detection of phase change with an equivalent sampling frequency of 400 MHz. These interpolated data were processed using software (LabVIEW, National Instruments, TX, USA) and the distance from the probe to each point on the bone surface was calculated.

2.2. *Accuracy assessment of the echo tracking method using an aluminum panel*

With this echo tracking system, we first verified the accuracy of the displacement measured in vitro by an echo tracking system that has been newly developed for measurement of bone deformation. A flat panel of aluminum alloy (65 mm × 85 mm × 10 mm) was fixed to a stepping motor (PK566-A: Oriental motor Co. Ltd., Tokyo, Japan) via a columnar support (TSL120: Nippon Thompson Co. Ltd., Tokyo, Japan) with its surface vertical to the driving axis. To direct ultrasound vertically toward the center of the panel, a 7.5 MHz linear electronic echo probe (UST-5710-7.5: Aloka Co. Ltd., Tokyo, Japan) was fixed to a custom-made probe stand (Aloka Co. Ltd., Tokyo, Japan). The echo probe and the aluminum panel were mounted independently from each other and the distance between them was set at 10 mm in the water bath. The panel was immersed in a plastic water tank (538 mm × 680 mm × 400 mm) and was translated distally along the direction of the echo beam at a displacement rate of 500 μm/s using the stepping motor. The displacement of a central point of the panel surface was measured by the echo tracking system. The displacement of the panel was also measured simultaneously by a linear potentiometer (AT-104: Keyence Corporation, Osaka, Japan) with a proven accuracy of 1 μm at the flat surface of the columnar support above the water (Fig. 3A and B). The accuracy of the echo tracking system was evaluated by comparing these two measurements and the standard deviation (S.D.) of the difference between the displacement measured by the echo tracking and by the potentiometer was calculated. The data-sampling rate for the echo tracking system was 500 Hz and that for the potentiometer was 100 Hz. Throughout the experiment, the water temperature was kept at 24 °C.

2.3. *A three point bending test using a porcine tibia with both ends fully constrained*

To evaluate how accurately the echo tracking system detect bone deformation under loading by monitoring displacement

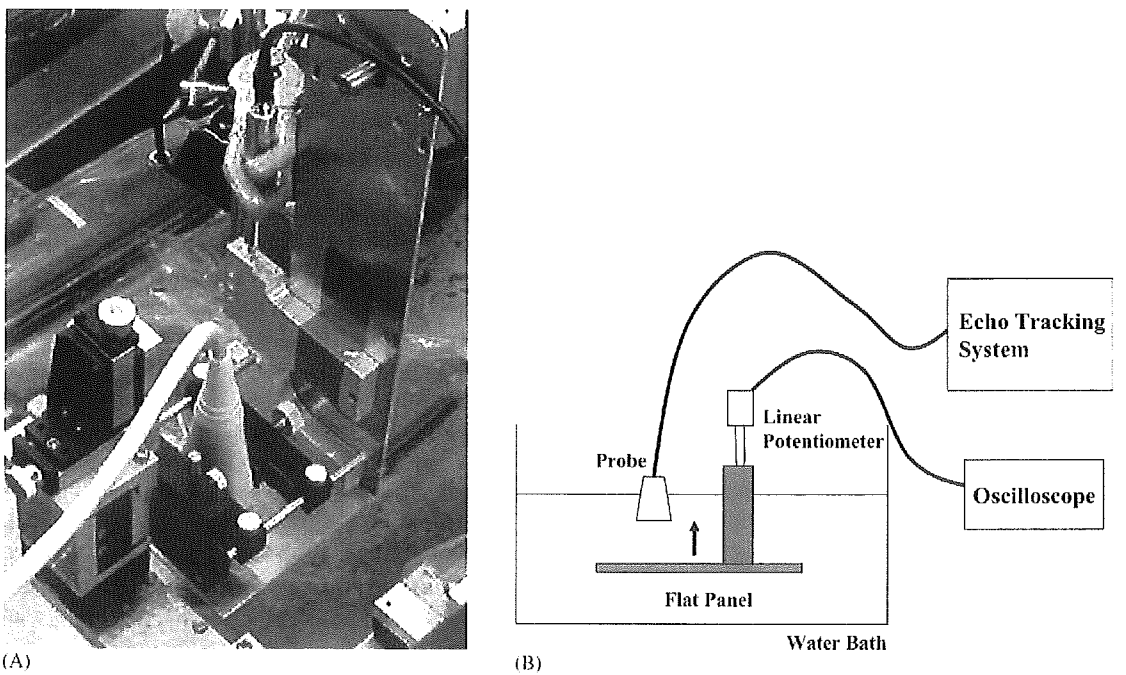

Fig. 3. (A and B) A flat panel fixed to a stepping motor via a columnar support in a plastic water tank vertically moved towards a 7.5 MHz linear electronic echo probe at a displacement rate of 500 μm/s. The displacement of a central point on the panel surface was measured by the echo-tracking system. The displacement of the panel was also measured simultaneously by a linear potentiometer.

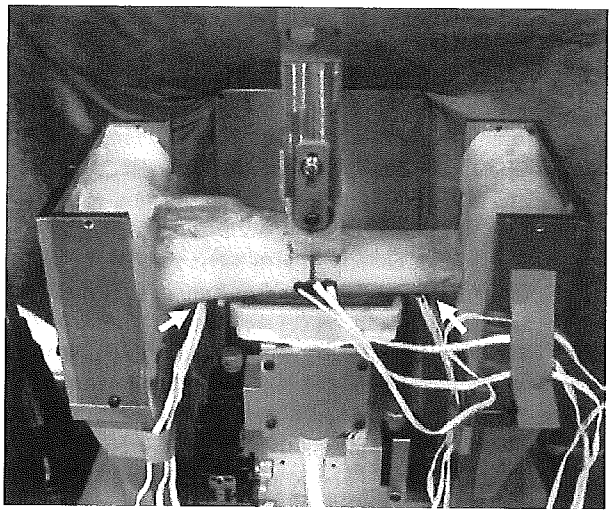

Fig. 4. After removing the soft tissues, the tibia was placed with its medial aspect upwards and both ends of the tibia were fully constrained with dental resin with a span of 214 mm. Two strain gauges were attached to the posterior aspect of the tibia at 50 mm proximal and 50 mm distal from the center of the tibia respectively. Displacement of the osseous surface was measured with the 7.5 MHz linear probe throughout the loading process and strain at each of the gauge sites was simultaneously measured. A single-cycle load and a three-cycle load were applied. (The white arrow on the left indicates the location of proximal strain gauge attached to the posterior bone surface and the white arrow on the right indicates the distal strain gauge.)

of the point on the bone surface, a three-point bending test using a porcine tibia was also performed to measure displacement at the surface of the tibia with the same echo tracking system. An adult porcine tibia with a length of 260 mm (preserved freshly frozen) was used for this experiment. After removing the soft tissues, the tibia was placed horizontally on a testing machine (Tensilon UTM-2.5T: A&D Co. Ltd., Tokyo, Japan) with its medial aspect upwards and both ends of the bone were fully constrained by dental resin (GC Ostron2®: GC, Tokyo, Japan) with a span of 214 mm. Two rosette strain gauges (KGF-1: Kyowa Electronic Instruments, Tokyo, Japan) were attached to the posterior aspect of the tibia at 50 mm proximal and 50 mm distal from the center of the bone respectively. The displacement at the center of the bone surface was measured with the same probe throughout the loading process and the maximum principal strain at each of the gauge sites was measured simultaneously. A single-cycle load and a three cycle-load from 0 to 5780 N were applied at the center of the span of 214 mm in the lateral-medial plane using a resin pusher with a thickness of 25 mm and an actuator speed of 0.1 mm/s over a distance of 0.7 mm (Fig. 4). The sampling rate for the echo tracking system was 500 Hz and that for the strain gauges was 100 Hz. The room temperature was kept at 22 °C and the tibia was kept moistened with physiological saline throughout the experiment. The maximum principal strain measured by the two strain gauges was compared with the displacement shown by the echo tracking system.

2.4. A multi-echo tracking system

We also developed another echo tracking system (multi-echo tracking system) that was capable of simultaneously tracking multiple points. Five points were set along the long axis of the probe at intervals of 10 mm. Displacement at each of the five points was measured simultaneously, and surface deformation of the bone was shown as a third order spline complement curve defined by the displacement at the five points measured by the echo tracking system. The echo tracking system strain (ETS) was calculated by the following equation as a parameter of surface deformation.

$$\mathrm{ETS} = D/L \tag{1}$$

where L is the distance from the first tracking point to the fifth point, and D is the maximum distance from the spline curve to a straight line connecting the first and fifth tracking points. With this multi-echo tracking system, it is assumed that the displacement caused by translation to the direction of the echo beam and rotation in the plane including a loading point and five tracked points, is cancelled.

2.5. A three point bending test with proximal and distal metaphyses supported

To prove the multi-echo tracking system could detect bone deformation even when the measured object underwent some translation, we also measured the deformation of a porcine tibia. After the soft tissues were removed, the tibia with a length of 230 mm was placed horizontally on the testing machine (Servo Pulser, Shimadzu Corporation, Tokyo, Japan) with its medial aspect upwards and both sides of the metaphyses were supported by rollers with a span of 115 mm. A three-point bending load was applied by a resin pusher with a width of 25 mm at the mid point between the two supporting rollers (Fig. 5). Deformation and strain on the posterior surface of the tibia were measured simultaneously with a 7.5 MHz linear probe and two strain gauges (KGF-1, Kyowa, Tokyo, Japan). Five tracking points were set along the long axis of the tibia with the third point corresponding to the site of loading. The echo probe was fixed parallel to the posterior surface of the tibia at a distance of 20 mm. Two strain gauges were attached along the tracking line (a straight line formed by the five tracking points) at 5 mm distal and 5 mm proximal to the third point (center point) and with each gauge axis parallel to the tracking line. The gauge surfaces were waterproofed by coating tar (The Yokohama Rubber Company, Tokyo, Japan). Incremental load increases were applied from a preload of 100 N up to 1500 N. The loading rate was set at 25 N/s. Under each load, the ETS value and the readings of the two strain gauges set parallel to the tracking line were determined. The data sampling rate for echo tracking was 100 Hz and that for the strain gauges was 100 Hz. The correlation between the ETS value and each of the strain gauge readings was calculated with Pearson's cor-

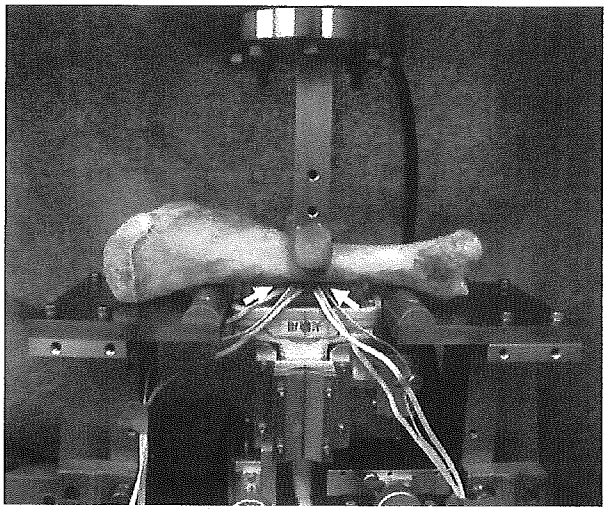

Fig. 5. The extracted porcine tibia was placed horizontally on the testing machine with a medial aspect upwards and both sides of the metaphysis were supported by rollers. Three-point bending loads were applied by a resin pusher from a preload of 100 N up to 1500 N. Deformation and strain of the posterior surface of the tibia were simultaneously measured with a 7.5 MHz linear probe and two strain gauges. Two strain gauges were attached to the tracking line at 5 mm distal and 5 mm proximal to the third tracking point with each gauge axis parallel to the tracking line. The gauge surfaces were waterproofed by coating tar. (The white arrow on the left indicates the location of proximal strain gauge attached to the posterior bone surface and the white arrow on the right indicates the distal strain gauge.)

relation analysis. The room temperature was kept at 22 °C and the tibia was kept moistened with physiological saline throughout the experiment. The sound speed used for the echo tracking measurement was set from the temperature of water in a bath and a bag attached to the probe according to the equation for the relation between water temperature and sound speed proposed by Greenspan [11].

3. Results

For measurement of the displacement of the flat panel, there was excellent linearity between the data obtained by the echo tracking system and the linear potentiometer ($r = 0.999$). The standard deviation (S.D.) of the difference between the displacement measured by the echo tracking system and that measured by the potentiometer was ±2.6 μm.

In the three-point bending test of the porcine tibia, the maximum principal strain recorded by the strain gauge set at 50 mm proximal to the loading point under a load of 5780 N (the maximum load) was 1077 micro strain and that at 50 mm distal was 1350 micro strain, whereas the displacement measured by echo tracking was 678.5 μm. The strain gauge readings and those of the echo tracking system showed excellent linearity with a correlation coefficient of 0.999 for the proximal strain gauge and 0.996 for the distal gauge (Fig. 6). The curve relating the load magnitude with the data obtained from each strain gauge was a typical hysteresis loop, indicating the measured bone was a visco elastic material. The curve for the relationship between the load magnitude and the displacement of the echo tracking system was also a hysteresis loop (Fig. 7).

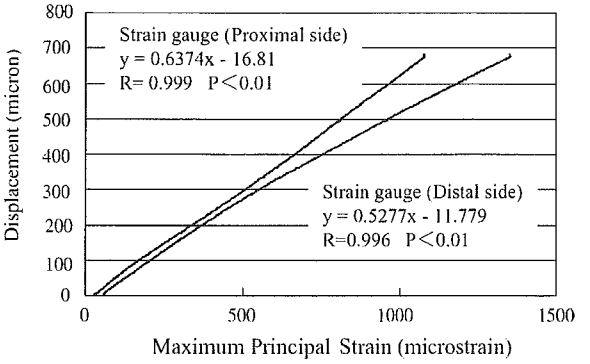

Fig. 6. Result of the single-cycle load in the three-point bending test of the porcine tibia. The graph showed that the strain gauge readings and those with the echo tracking system had an excellent linearity with a correlation coefficient of 0.999 and 0.996 all through the loading cycles.

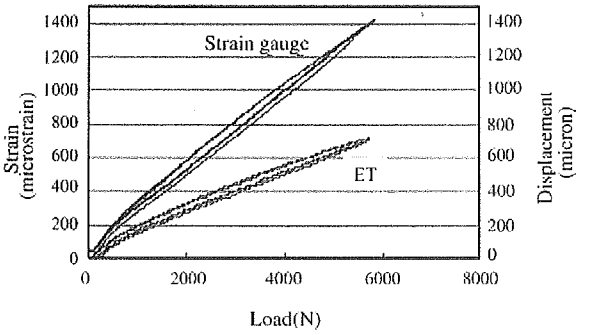

Fig. 7. Result of the three-cycle load in the three-point bending test of the porcine tibia. The curve relating the load magnitude with the data obtained from the strain gauge of the distal side was a typical hysteresis loop, indicating that the measured object was a viscoelastic material. The curve for the relationship between the load magnitude and the displacement of the echo tracking system was also a hysteresis loop.

In the study with the multi-echo tracking system, the strain readings of each gauge and the data from the entire system showed a perfect linear increase with the load. There was a linear relation between echo tracking data and each of the strain gauges ($r = 0.998$ and 0.998, respectively) (Fig. 8A and B). The reading for the gauge axis parallel to the tracking line and the maximum principal strain on the distal gauge at 1500 N was 1154.6 and 1160.4 micro strain, respectively. The angle of the direction of the maximum principal strain was 7° with reference to the echo tracking line.

4. Discussion

Bone shows deformation in response to an applied load. By quantitatively measuring this deformation, it is possible to assess the mechanical properties of bone material. Because

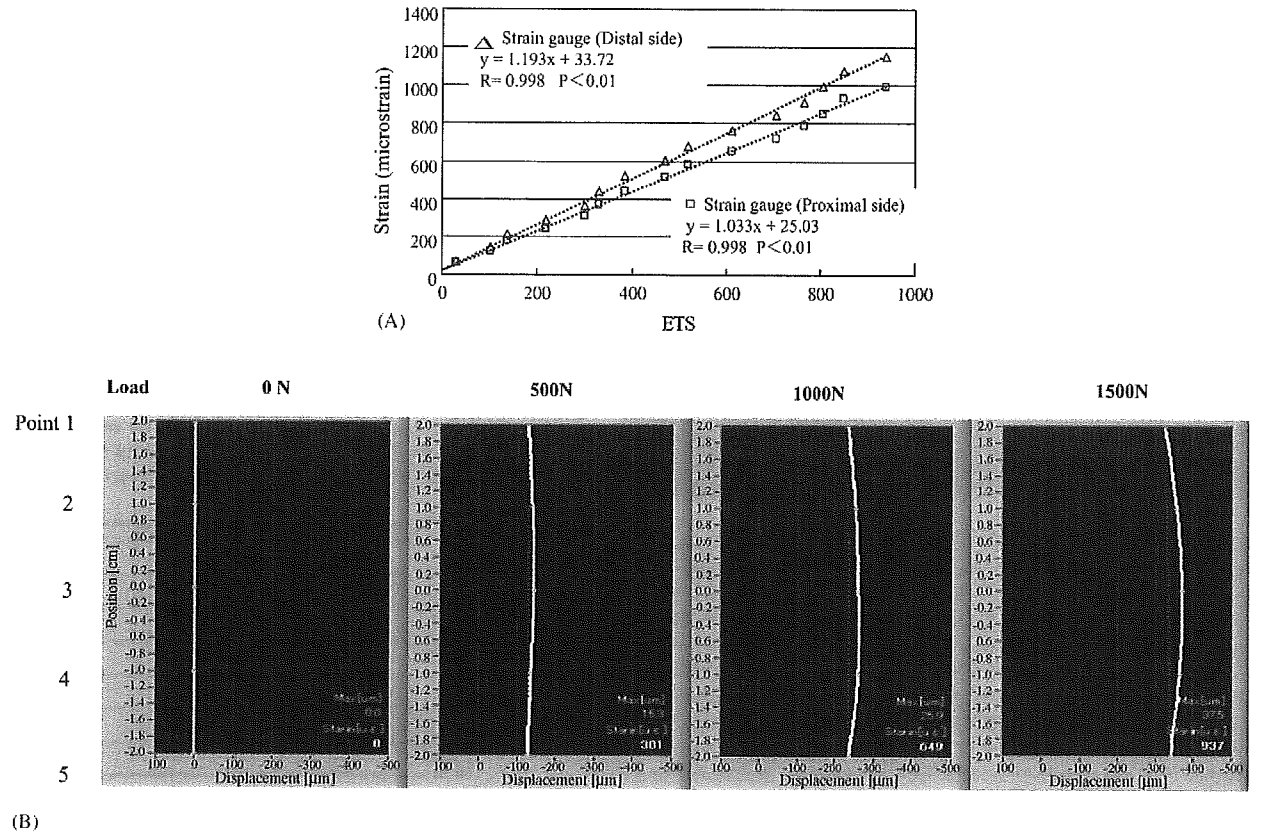

Fig. 8. (A) Result of the three-point bending test of the porcine tibia with the multi-echo tracking system. The strain readings of each gauge and the data from the entire system showed a perfect linear increase with the load. There was a linear relation between echo tracking data and each of the strain gauges ($r = 0.998$ and 0.998, respectively). (B) Result of the displacements at the five tracked points under the loads of 0, 500, 1000 and 1500 N. The surface deformation was visualized by a third order spline complement curve. The surface deformation increased with the increase of the load.

bone is a viscoelastic material, we can estimate its strength by measuring the elasticity, viscosity, and plasticity under dynamic loading. In this study, we attempted to develop an echo tracking method to noninvasively detect bone deformation under a load.

Numerous quantitative measurement methods using ultrasound have been tested to evaluate the elastic properties of bone or the fracture risk [12]. The axial transmission technique was based on the propagation of guided ultrasound waves along the bone surface. A set of ultrasound transducers (transmitters and receivers) was placed on the skin along the bone to measure the velocity of ultrasound waves passing through the cortical layer of the bone parallel to its axis. Sievanen et al. [13] reported in their study of the axial transmission technique that the cortical density was the only determinant of speed of sound measured in the radial and tibial shafts in vivo. The technique of measuring broadband ultrasound attenuation (BUA) and sound of speed (SOS) for the calcaneus was recently developed. Ultrasound transmitted to the calcaneus penetrates the bone and is detected by the receiver located on the opposite side. Then the stiffness of the bone is calculated from the measured BUA and SOS values. This stiffness index is reported to be closely correlated with the regional bone mineral density measured by dual energy X-ray absorptiometry (DXA) [14]. These methods of quantitative evaluation by ultrasound technology have been based on measurement of the speed, permeability, and attenuation of ultrasound transmitted through the bone. In this respect, the echo tracking method that measures bone deformation differs markedly from these preceding ultrasound techniques.

Ultrasonography can clearly visualize the bone surface because the acoustic impedance of osseous tissue differs greatly from that of the surrounding soft tissues. However, the spatial resolution of B-mode images is not better than 100 μm. Therefore, measurement of bone deformation from B mode images is thought to lack sufficient precision, because resolution of better than 10 μm is considered to be necessary to detect deformation compatible to that measured by a strain gauge, which can detect deformation of 0.001 μm when the gauge length is 1 mm (the smallest available gauge). Thus, much more accurate measurement technology has been needed. Measurement of bone surface displacement using the echo tracking fulfils this requirement. The echo tracking method currently used for measuring arterial wall motion has an accuracy of one-sixteenth of a wave length, which is an accuracy of 13 μm at every 1 mm/s with a 7.5 Hz probe. The

system was further improved to measure minute displacement of the bone and a much better precision of 2.6 μm could be obtained by improving the software to utilize the characteristics of the acoustic impedance of bone, so that minute displacement of tracked points on the bone surface could be measured.

The purpose of the first three-point bending test in which both ends were fully constrained was to evaluate whether the echo tracking system could in fact detect bone deformation accurately because the surface of bone was not flat and there was a possibility of the surface morphology changing when deformed. The accuracy of the system was assessed by directly comparing the data from our echo tracking method with those simultaneously recorded by the strain gauges. In this experiment, bone deformation should be regulated to occur in the direction of the echo beam. Because the probe was mounted firmly by an external support and faced the direction of loading, the echo tracking system could only detect displacement in the beam direction. The system used in this experiment could only detect displacement of a single point, so translation of the measured object should have been avoided. From the result of the experiment, we could prove that the correlation between the strain-related data from the echo tracking and the strain gauge readings was excellent. Therefore, the echo tracking method provided sufficient accuracy for detection of bone surface deformation.

Under a cyclic load, the system was able to monitor bone viscoelasticity because the load versus displacement curve was a hysteresis loop. It is well known that bone shows vicsoelasticity, but its nature has not been sufficiently investigated in vivo, because few techniques have been available to assess bone viscoelasticity in vivo. Only Moorcroft et al. [15] and Ohnishi et al. [16] have already investigated viscoelasticity in vivo using an external fixation system. To date, no method has been available to noninvasively assess the viscoelasticity of bone in vivo. However, it is very useful to assess bone viscoelasticity because it varies markedly during the process of fracture healing. The hysteresis loop shown by the echo tracking method indicated that it could be used to quantitatively assess in vivo viscoelasticity noninvasively in the future. Further investigations using bone models of known viscoelasticity will be needed to confirm the precision of the echo tracking system.

The purpose of the second three-point bending test in which both sides of the metaphyses were supported by rollers was to prove that the echo tracking system could detect bone deformation even when the measured object underwent some translation. Measurement of only one point is inadequate for detecting deformation because the displacement caused by translation of a moving object will be mixed. Accordingly, measurement of multiple points should be necessary to cancel the displacement caused by translation. Using the system with the multiple tracked points set along the straight line, it is assumed that the displacement caused by translation to the direction of the echo beam and rotation in the plane including the loading point and the five tracked points is cancelled. The test in which both metaphyses were simply supported by rollers allows the tibia to translate to the direction of loading and to rotate within the frontal plane (the plane that includes the loading point and both supporting points). The magnitude of the strain measured by the strain gauges was an average strain of 1 mm gauge length, while the ETS measured an average strain of 40 mm. However, the linearity of both methods was very strong, indicating that only deformation components from the displacement data of five tracked points could be extracted even when the measured object underwent some translation. The strain along the tracking line was very close to the maximum principal strain and the difference in the direction of both was very small (only 7°). This indicated that the direction of strain at the center of the posterior surface of the tibia generated by three-point bending was almost parallel to that of the echo tracking line. By echo tracking measurement of multiple points, it is possible to optimize the detection environment depending on the pattern or mode of bone deformation under specific mechanical conditions by changing the interval and number of the measured points.

Our method has the technical limitation of only detecting deformation in the plane that includes the measured points because the tracking points were all located on a straight line. When bone deformation occurs in multiple planes, only the component of deformation in the measured plane can be detected, and the other components cannot be measured with the current system. To overcome this limitation, a measurement system should be developed with a three-dimensional distribution of multiple tracking points that is capable of detecting multi-directional deformation.

Our echo tracking system had sufficient accuracy to detect bone surface deformation and could monitor the viscoelasticity of bone. Although further investigations will be necessary before this method can be applied to in vivo measurement, our echo tracking method might have a considerable potential for noninvasive measurement of the viscoelasticity and plasticity of bone.

Acknowledgement

This work was funded in part by the grant from the Pharmaceutical and Medical Devices Agency of Japan.

References

[1] Hung CT, Allen FD, Pollack SR, Brighton CT. Intracellular Ca^{2+} stores and extracellular Ca^{2+} are required in the real-time Ca^{2+} response of bone cells experiencing fluid flow. J Biomech 1996;29(11):1411–7.

[2] Johnson DL, McAllister TN, Frangos JA, Frangos JA. Fluid flow stimulates rapid and continuous release of nitric oxide in osteoblasts. Am J Phys 1996;271(1Pt1):E205–8.

[3] Reich KM, Frangos JA. Effect of flow on prostaglandin E2 and inositol trisphosphate levels in osteoblasts. Am J Phys 1991;261(3Pt1): C428–32.

[4] Fritton SP, Rubin CT, in: Cowin SC (Ed.), In Vivo Measurement of Bone Deformations Using Strain Gauges. Bone Mechanics Hand Book 8-1, 2nd ed.
[5] Jernberger A. Measurement of stability of tibial fractures. A mechanical method. Acta Orthop Scand 1970;135(Suppl):1–88.
[6] Gail PP, Brian LD, Amy CC, Sudan EDA. An extensometer for global measurement of bone strain suitable for use in vivo in humans. J Biomech 2001;34(3):385–91.
[7] Burr DB, Milgrom C, Fyhrie D, Furwood M, Nyska M, Finestone A, Hoshaw S, Saiag E, Simkin A. In vivo measurements of human tibial strains during vigorous activity. Bone 1996;18(5):405–10.
[8] Lanyon LE, Hampson WGJ, Goodship AE, Shah JS. Bone deformation recorded in vivo from strain gauges attached to the human tibial shaft. Acta Orthop Scand 1975;46:256–68.
[9] Hokanson DE, Mozersky DJ, Sumner DS, Strandness DEJ. A phase-locked echo tracking system for recording arterial diameter changes in vivo. J Appl Physiol 1972;32(5):728–33.
[10] Harada A, Okada T, Niki K, Chang D, Sugawara M. On-line noninvasive one-point measurements of pulse wave velocity. Heart Vessels 2002;17:61–8.
[11] Greenspan M. Tables of the speed of sound in water. J Acoust Soc Am 1959;31(1):75–6.
[12] Laugier P, Padilla F, Camus E, Chaffaï S, Chappard C, Peyrin F, Talmant M, Berger G. Quantitative ultrasound for bone status assessment. IEEE Ultrason Symp. 2000:1341–50.
[13] Sievanen H, Cheng S, Ollikainen S, Uusi-Rasi K. Ultrasound velocity and cortical bone characteristics in vivo. Osteoporos Int 2001;12(5):399–405.
[14] Cortet B, Boutry N, Dubois P, Legroux-Gerot I, Cotten A, Marchandise X. Does quantitative ultrasound of bone reflect more bone mineral density than bone microarchitecture? Calcif Tissue Int 2004;74(1):60–7.
[15] Moorcroft CI, Ogrodnik PJ, Thomas PBM, Wade RH. Mechanical properties of callus in human tibial fractures: a preliminary investigation. Clin Biomech 2001;16:776–82.
[16] Ohnishi I, Nakamura K, Okazaki H, Sato W, Kurokawa T. Evaluation of the fracture site mechanical properties in vivo by monitoring the motion of a dynamic pin clamp during simulated walking. Clin Biomech 2002;17(9/10):687–97.

Introduction

Most vertebral fractures among the elderly occur because of their skeletal fragility due to osteoporosis. To assess the risk of vertebral fracture and its prevention, it is essential to predict vertebral bone strength. Clinically, measurement of bone mineral density by quantitative computed tomography (QCT) and dual energy X-ray absorptiometry (DXA) have been used to predict vertebral strength. However, the correlations between vertebral strength and bone mineral density measured by QCT are reported to be 0.37-0.72 [1-5] and those with DXA are reported to be 0.51-0.80 [4-7]. Therefore, such methods only explain 40 to 80% of vertebral strength.

Finite element (FE) models based on data from QCT may predict vertebral strength more accurately because they assess geometry, architecture and heterogeneous mechanical properties of the bone. CT-based FE models are known to be able to make accurate predictions on fracture loads for femur [8-12]. For vertebra, there have been several attempts to predict fracture strength, and the correlations between compressive vertebral strength and predicted strength were reported to be high (r=0.89-0.95) [13-16]. However, the slopes of the regression line between the measured fracture loads and the predicted were much less than 1.0 (0.569-0.86) and no quantitative prediction could have been made with dependable accuracy. Furthermore, previous models did not compare the fracture sites within a whole vertebra. For clinical application, it is essential for a simulation method to be able to predict both vertebral

strength and fracture sites because these are the requisite predictors of a vertebral fracture.

Prediction of vertebral fracture has been difficult because of complex geometry, elastoplasticity, and thin cortical shell of the vertebra. The vertebra has elaborate architecture and geometry with curved surfaces, which cannot be realistically modeled with eight-noded hexahedron elements. Previous mechanical tests showed that there was a difference between tensile and compressive behavior of the bone [17-19]. The compressive behavior showed nonlinear behavior. Therefore, a nonlinear FE model should be utilized to predict the clinical fracture load.

The cortical shell of the vertebra is estimated to be thin with a thickness of less than 0.5 mm [20-22]. On the other hand, the resolution of a clinically available CT scanner is very low with a pixel spacing larger than 0.25 mm. With the currently available CT resolution, a thin cortical shell cannot be precisely modeled. The thickness tends to be overestimated and its density to be underestimated [23, 24]. Therefore, it would be necessary to construct a thinner part of the cortical shell from data that is independent of QCT data.

The purpose of this study was to establish a nonlinear FE model which predicted the vertebral strength and the fracture sites, and then to evaluate the accuracy of our FE model by performing mechanical testing with human cadaveric specimens.

Materials and Methods

Twelve thoracolumbar (T11, T12, and L1) vertebrae with no skeletal pathologies were collected within 24 hours of death from 4 males (31, 55, 67, and 83 years old). Causes of death for the four donors were myelodysplastic syndrome, pneumonia, adult T-cell leukemia, and bladder cancer, respectively. All of the specimens were obtained at University of Tokyo Hospital with the approval of our ethics committee and with informed consent. They were stored at –70 C° after each step in our protocol. The vertebrae were disarticulated, and the discs were excised. Then the posterior elements of each vertebra were removed by cutting through the pedicles.

The vertebrae were immersed in water and axial CT images with a slice thickness of 1 mm and pixel width of 0.351 mm were obtained using Lemage SX/E (GE Yokokawa Medical System, Tokyo, Japan) with a calibration phantom containing hydroxyapatite rods.

Nonlinear finite element analysis

The CT data were transferred to a workstation (Endeavor Pro-1000, Epson Direct Co., Nagano, Japan). The 3D FE models were constructed from the CT data using MECHANICAL FINDER software (Mitsubishi Space Software Co., Tokyo, Japan). Trabecular bone was simulated using 2 mm linear tetrahedral elements, and the outer surface of the cortical shell was modeled using 2 mm triangular-plates (Fig. 1). The thickness of the cortical shell was set

as 0.4 mm based on the previous papers [20-22]. On average there were 41,133 and 3,191 tetrahedron elements and triangular-plates, respectively.

To allow for bone heterogeneity, the mechanical properties of each element were computed from the Hounsfield unit value. Ash density of each voxel was determined from the linear regression equation created by these values of the calibration phantom. Ash density of each element was set as the average ash density of the voxels contained in one element. Young's modulus and yield stress of each tetrahedron element were calculated from the equations proposed by Keyak et al. [10]. Young's modulus of human vertebra cancellous tissue was reported as 3.8-13.4 GPa [25-28]; Young's modulus of each triangular-plate was set as 10 GPa. Poisson's ratio of each element was set as 0.4, which was used in the previous papers [10, 29].

A uniaxial compressive load with uniform distribution was applied on the upper surface of the vertebra and all the elements and all the nodes of the lower surface were completely restrained. The models were analyzed using MECHANICAL FINDER. A nonlinear FE analysis by Newton-Raphson method was utilized. To allow for the nonlinear phase, mechanical properties of the elements were assumed to be bi-linear elastoplastic, and the isotropic hardening modulus was set as 0.05, which is generally used in the analysis of concrete materials. Each element was assumed to yield when its Drucker-Prager equivalent stress reached the element yield stress. Failure was defined as occurring when the minimum